PB-244 403

STUDIES OF SMALL METALLIC PARTICLES FORMED BY HOMOGENEOUS NUCLEATION -- LIGHT SCATTERING AND ELECTRON MICROSCOPY

Jay D. Eversole, et al

California University

Prepared for:

Environmental Protection Agency

February 1975

DISTRIBUTED BY:

NTIS

National Technical Information Service
U. S. DEPARTMENT OF COMMERCE

248029

EPA-650/3-75-006

February 1975

PB244403

Ecological Research Series

Reproduced by
NATIONAL TECHNICAL
INFORMATION SERVICE
U S Department of Commerce
Springfield VA 22151

TECHNICAL REPORT DATA
(Please read Instructions on the reverse before completing)

1. REPORT NO.	2.	3. PB 244 403
EPA-650/3-75-006		

4. TITLE AND SUBTITLE	5. REPORT DATE
Studies of Small Metallic Particles Formed by Homogeneous Nucleation — Light Scattering and Electron Microscopy	FEBRUARY, 1975
	6. PERFORMING ORGANIZATION CODE
7. AUTHOR(S)	8. PERFORMING ORGANIZATION REPORT NO.
Jay D. Eversole, Paul K. Hansma and H. P. Broida	
9. PERFORMING ORGANIZATION NAME AND ADDRESS	10. PROGRAM ELEMENT NO.
Department of Physics University of California Santa Barbara, California 93106	1AA008
	11. CONTRACT/GRANT NO.
	Grant No. R-800845
12. SPONSORING AGENCY NAME AND ADDRESS	13. TYPE OF REPORT AND PERIOD COVERED
Office of Research and Monitoring U. S. Environmental Protection Agency Washington, D. C. 20460	Final Report, 3/72 - 2/75
	14. SPONSORING AGENCY CODE

15. SUPPLEMENTARY NOTES

16. ABSTRACT

This report describes basic research on the subject of formation and detection of metallic particles ranging from 5 to 5000 nm in diameter. Particulate matter is formed in a flowing inert gas by homogeneous nucleation from the vapor phase. Metals used in the work done under this grant include Na, K, Li, Rb, Cs, Cd, Mg, Zn, and Pb. Specific objectives of this project are necessarily broad and open-ended as present understanding of particle formation and growth mechanism is still in an early state of development. Particulate matter with diameters less than 100 nm plays an important role in atmospheric pollution, and it was hoped that research would contribute to the detection, measurement, and/or control of this problem.

Observations of plasma-resonance scattering of white light from alkali metal particles, the growth of Zn particles observed by electron microscopy, and the development of a superconducting device: a small-particle Josephson magnetometer, are significant results of this project which have been published. Attempts to observe the Raman scattering of laser light from Zn, Mg, and Cd particles, to isolate macroscopic quantities of particles from the flow system, and to obtain information from the 0 to 180 degrees angular light scattering were not totally successful.

17. KEY WORDS AND DOCUMENT ANALYSIS

a. DESCRIPTORS	b. IDENTIFIERS/OPEN ENDED TERMS	c. COSATI Field/Group
particulate particle nulceation plasma-resonance sodium (Na); potassium (K); zinc (Zn)	PRICES SUBJECT TO CHANGE	

18. DISTRIBUTION STATEMENT	19. SECURITY CLASS (This Report)	21. NO. OF PAGES
Release Unlimited	Unclassified	48
	20. SECURITY CLASS (This page)	22. PRICE
	Unclassified	$3.75 - 2.25

EPA Form 2220-1 (9-73)

EPA-650/3-75-006

STUDIES OF SMALL METALLIC PARTICLES FORMED BY HOMOGENEOUS NUCLEATION: LIGHT SCATTERING AND ELECTRON MICROSCOPY

by

H. P. Broida, J. D. Eversole,
and P. K. Hansma

University of California
Santa Barbara, California 93106

Grant No. 800845
Project No. 21AJX-004
Program Element No. 1AA008

EPA Project Officer: Dr. Jack L. Durham

Chemistry and Physics Laboratory
National Environmental Research Center
Research Triangle Park, North Carolina 27711

Prepared for

U. S. ENVIRONMENTAL PROTECTION AGENCY
OFFICE OF RESEARCH AND DEVELOPMENT
WASHINGTON, D. C. 20460

ja
February 1975

EPA REVIEW NOTICE

This report has been reviewed by the National Environmental Research Center – Research Triangle Park, Office of Research and Development, EPA, and approved for publication. Approval does not signify that the contents necessarily reflect the views and policies of the Environmental Protection Agency, nor does mention of trade names or commercial products constitute endorsement or recommendation for use.

RESEARCH REPORTING SERIES

Research reports of the Office of Research and Development, U.S. Environmental Protection Agency, have been grouped into series. These broad categories were established to facilitate further development and application of environmental technology. Elimination of traditional grouping was consciously planned to foster technology transfer and maximum interface in related fields. These series are:

1. ENVIRONMENTAL HEALTH EFFECTS RESEARCH
2. ENVIRONMENTAL PROTECTION TECHNOLOGY
3. ECOLOGICAL RESEARCH
4. ENVIRONMENTAL MONITORING
5. SOCIOECONOMIC ENVIRONMENTAL STUDIES
6. SCIENTIFIC AND TECHNICAL ASSESSMENT REPORTS
9. MISCELLANEOUS

This report has been assigned to the ECOLOGICAL RESEARCH series. This series describes research on the effects of pollution on humans, plant and animal species, and materials. Problems are assessed for their long- and short-term influences. Investigations include formation, transport, and pathway studies to determine the fate of pollutants and their effects. This work provides the technical basis for setting standards to minimize undesirable changes in living organisms in the aquatic, terrestrial, and atmospheric environments.

This document is available to the public for sale through the National Technical Information Service, Springfield, Virginia 22161.

Publication No. EPA-650/3-75-006

ABSTRACT

This report describes basic research on the subject of formation and detection of metallic particles ranging from 5 to 5000 nm in diameter. Particulate matter is formed in a flowing inert gas by homogeneous nucleation from the vapor phase. Metals used in the work done under this grant include Na, K, Li, Rb, Cs, Cd, Mg, Zn,and Pb. Specific objectives of this project are necessarily broad and open-ended as present understanding of particle formation and growth mechanism is still in an early state of development. Particulate matter with diameters less than 100 nm plays an important role in atmospheric pollution, and it was hoped that research would contribute to the detection, measurement, and/or control of this problem.

Observations of plasma-resonance scattering of white light from alkali-metal particles, the growth of Zn particles observed by electron microscopy, and the development of a superconducting device: a small-particle Josephson magnetometer, are significant results of this project which have been published. Attempts to observe the Raman scattering of laser light from Zn, Mg, and Cd particles, to isolate macroscopic quantities of particles from the flow system, and to obtain information from the 0 to 180 degrees angular light scattering were not totally successful.

CONTENTS

		Page
Abstract		iii
List of Figures		v
Sections		
I	Conclusions	1
II	Introduction	2
III	Experimental Apparatus	5
IV	Plasma Resonance Light Scattering from Alkali Metal Particles	11
V	Electron Microscopy of Zn Particles	19
VI	Small Particle Josephson Magnetometer	31
VII	Observations of Laminar Flow in a Glass Tube	35
VIII	"Matrix" Isolation of Na Particles	36
IX	Raman Scattering	37
X	Summary	38
XI	References	39
XII	List of Publications	41

FIGURES

No.		Page
1.	Vacuum System Schematic	6
2	Standard Furnace Schematic	9
3	High Temperature Furnace Schematic	10
4	Scattered Light Spectra of Na	13
5	Scattered Light Spectra of K and Rb	15
6	Observation Chamber and Particle Collecting Apparatus Schematic	20
7	Zn Particles 1200 nm across	22
8	Indented Side views of Zn Particles	24
9	Summary of Three Size Categories of Zn Particles	25
10	Example of Agglometated Particle	27
11	Results of O_2 Contamination	28
12	The Smallest Size Range of Particles Observed	30
13a	Magnetic Field Dependence of the Critical Current of a Small Particle Array	32
b	Magnetic Field Dependence of the Critical Current of Two Coupled Small Particle Arrays	32

SECTION I

CONCLUSIONS

Identification of particle-composition by plasma-resonance light scattering, or by Raman scattering from the particles is not considered feasible with present state-of-the-art techniques for industrial or commercial applications. Correlation of plasma-resonance light scattering data to electron microscopy may provide important information on the fundamental processes of particle nucleation and growth. Optical structure should also exist for certain semiconductor materials arising from interband transitions rather than plasma-resonance which again would provide basic information rather than direct application.

Relative concentrations of carbon-based particles could conceivably be measured utilizing plasma resonance light scattering. However, more research is required to make a definate statement on this possibility.

SECTION II

INTRODUCTION

GENERAL

One result of current industrial activity in the United States has been the introduction of approximately 10^7 tons per year of particulate matter into the atmosphere.[1] Current particulate air pollution is very much in evidence as can readily be seen in industrial smoke emissions and in the turbidity of the atmosphere in the vicinity of cities. Of the emitted particles, the smaller, less visible particles in the size range below 0.1 μ are the most difficult to control and detect. These very small particles have received little attention as to creation, detection and control.[1-5]

The increase in the number of very small particles over the natural background level, characteristic of cities, seems to be entirely the result of combustion. Examining some cases where particle size has been measured at the particles source, Silverman, et al.[6] have found that, by number, the majority of particles emitted by an open hearth furnace are below 100 nm diameter. Lee, et al. are cited[3] as finding that 90% by weight of automobile exhaust lead is emitted in the form of particles with diameters less than 500 nm. It is possible that any process of incineration or combustion that is able to vaporize metals or metallic impurities may produce very small metallic or metallic oxide particles.

Atmospheric particles are routinely monitored in many cities using methods such as high-volume samplers, tape samplers, or turbidity measurements.[1-5] In general, these present monitoring methods emphasize the larger, more massive fraction of particles of sizes greater than 1000 nm. Subsequent measurements of the chemical composition of collected material, of course, tends again to emphasize the more massive materials, which may not be indiciative of the majority of particles.

At present, no reliable optical method exists for characterizing particles less than 100 nm diameter and the only direct method in use is the electron microscope after collection.[3,7] Other less direct methods such as observing condensation of water vapor on small particles after rapid expansion[8,9] and measurements of mobility of charged particles in an electric field[10] have been used for observing and characterizing very small particles.

These very small particles which have been somewhat ignored by present observational techniques are nevertheless important for the following reasons: 1) Because of their small size, very small particles have settling velocities on the order of 10^{-5} cm/sec and consequently have large residence times in the atmosphere. 2) Very small primary particles can escape control efforts at the source and subsequently grow to become larger particles either through direct combination or by participation in photochemical reactions. 3) Very small particles may be more injurious to health because they can be transported to the pulmonary and tracheobronchial regions of the respiratory tract, whereas larger particles can be deposited in the nasopharyngeal region where they can be removed by cilary action.[3,11]

One of the basic factors that has hampered studies of particles, especially growth mechanisms, has been the inability to generate particles in a controlled manner. At Santa Barbara, we have developed a method for producing metallic particles from a metal vapor flowing in a controlled atmosphere at temperatures from 300 to 2000 K. In initial studies, particles have been produced with sizes ranging from 5 to 1000 nm of the following materials: Pb, Zn, Na, K, Rb, Cs, Mg, Cd and Li.

Measurements and detection of particles less than 100 nm diameter in our system have been made using white light or laser light scattering and electron microscopy. In the case of very small metallic particles,

a maximum in the white light scattered intensity as a function of wavelength is seen, corresponding to plasma resonance of the conduction electrons of the particles. This scattered light is highly polarized. The wavelength and shape of the plasma resonance scattering should depend on the material, size, and shape of the particles.

SECTION III

EXPERIMENTAL APPARATUS

GENERAL

Particles are produced by evaporating bulk metal in a heated flowing inert gas. When the gas carries metal vapor to a cooler region of the flow system, a supersaturated condition of the metal vapor can be produced. At sufficiently low temperature, spontaneous condensation of small "solid" particles can result. Electron microscopy of such particles shows size ranges foom 5 to 5000 nm, depending on the production and collecting conditions of the system.

The experimental apparatus is illustrated in Fig. 1. The basic system consists of a furnace where the metal of interest is heated, and an observation chamber above the furnace where the particles are formed. Both of these are enclosed in, and partly made up of a vacuum flow system. It is convenient to describe the apparatus by separating these elements and discussing first, the vacuum flow system; and second, the furnace.

VACUUM FLOW SYSTEM

Vacuum flow systems are constructed from commercially manufactured stainless-steel tubing available in 5 and 10 cm diameters. "O-ring" grooves are cut into flanges on the ends of these pieces so that different pieces may be joined together with a vacuum seal by simply placing an "O-ring" between them. Special thumb-screw clamps hold the pieces in place. The stainless steel tubing may be obtained as crosses, tees, ells, weldable ferrules, and blank-offs; so that a great variety of configurations may be quickly and easily constructed.

Modifications necessary for valves, windows, pressure gauges, copper tubing adapters, flexible vacuum lines, and pump flanges are straignt-forward and simple shop work with the purchased blank-offs and weldable ferrules. The entire vacuum system therefore, becomes standardized

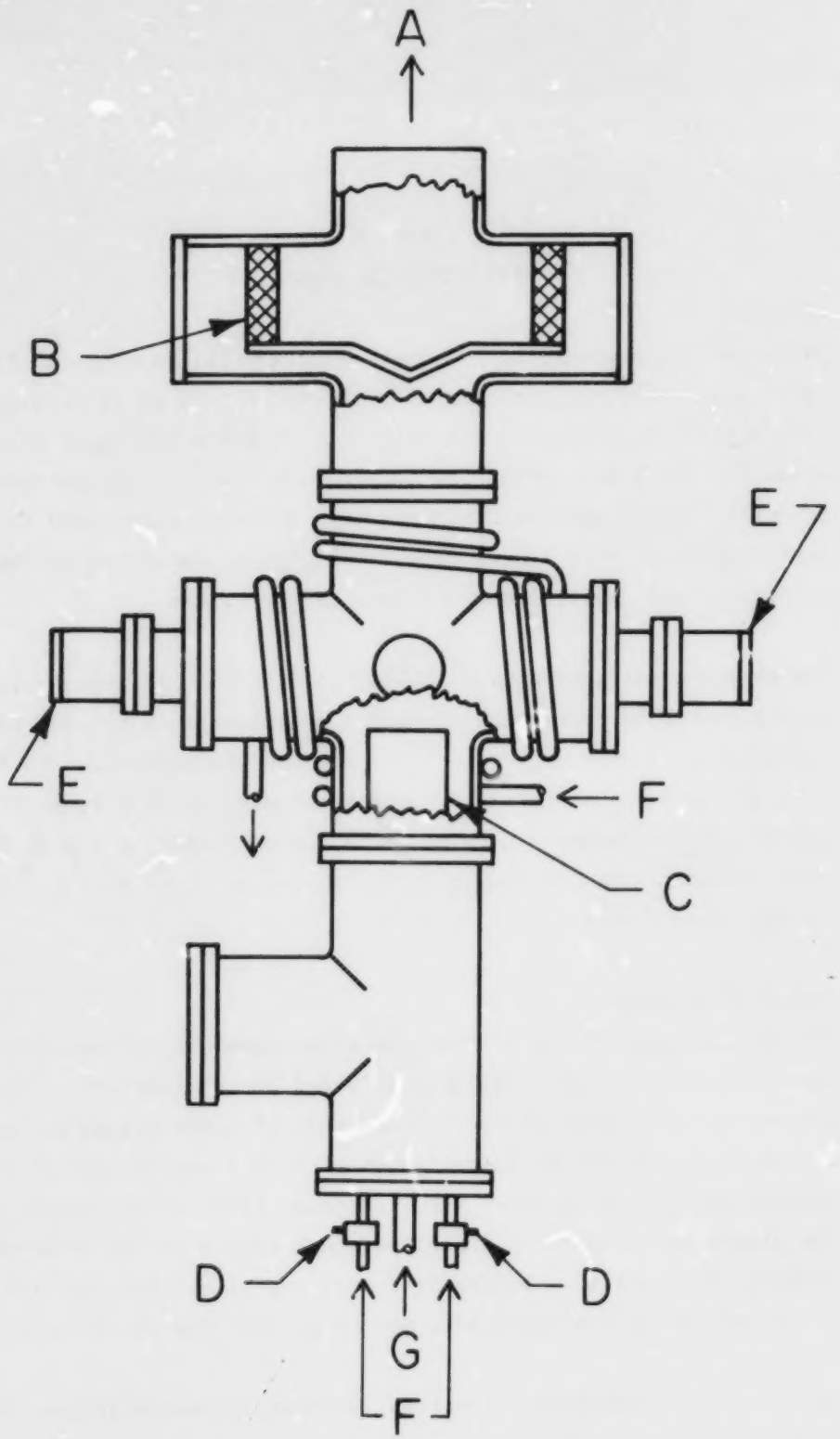

Fig. 1 Vacuum system schematic: A) to vacuum pump, B) filter, C) furnace, D) heater electrical contacts, E) windows, F) cooling water ports, and G) carrier gas inlet.

to 5 and 10 cm components with the flange, "O-ring", and clamp seal. The in-line filter assembly is the only part which is necessary to completely fabricate.

The central part of the apparatus is a 10 cm 4-way cross which forms the observation chamber. This cross has been modified by adding two 5 cm ferrules to form a 6-way cross. (See Fig. 1). The furnace protrudes into the bottom of this observation chamber and different housing is required below this cross depending on which furnace is used. In the horizontal plane the observation chamber will typically have three windows and a butterfly valve connected. The top port of the cross connects to the vacuum pump via a filter, valve, pressure gauge, and flexible vacuum hose. Apparatus for taking samples for electron microscopy may be attached to the other side of the butterfly valve, and this will be discussed in Section V. (See Fig. 6).

FURNACE

The standard furnace design could achieve a maximum temperature of 900°-1000°C. In later designs temperatures in the 1600°-1800°C range were reached, hence a distinction between the "standard" and "high temperature" furnaces must be made. However, in both types of furnaces, there is the basic design of an indirectly heated crucible. The major difference is that higher tempteratures were achieved in part by a smaller size to minimize conduction losses, so that the component size of the high-temperature furnace is less than half the scale of the standard furnace. In both cases an alumina crucible containing the metal of interest is supported inside an alumina tube, and this outer tube is heated electrically by a tungsten wire. Heat is transferred from the wall of the tube to the crucible by the inert carrier gas introduced at the bottom of the tube. The mixture of carrier gas and metal vapor exits through a nozzle at the top of the tube to the observation region. Cooling occurs because of conduction to the walls, which are at room temperature.

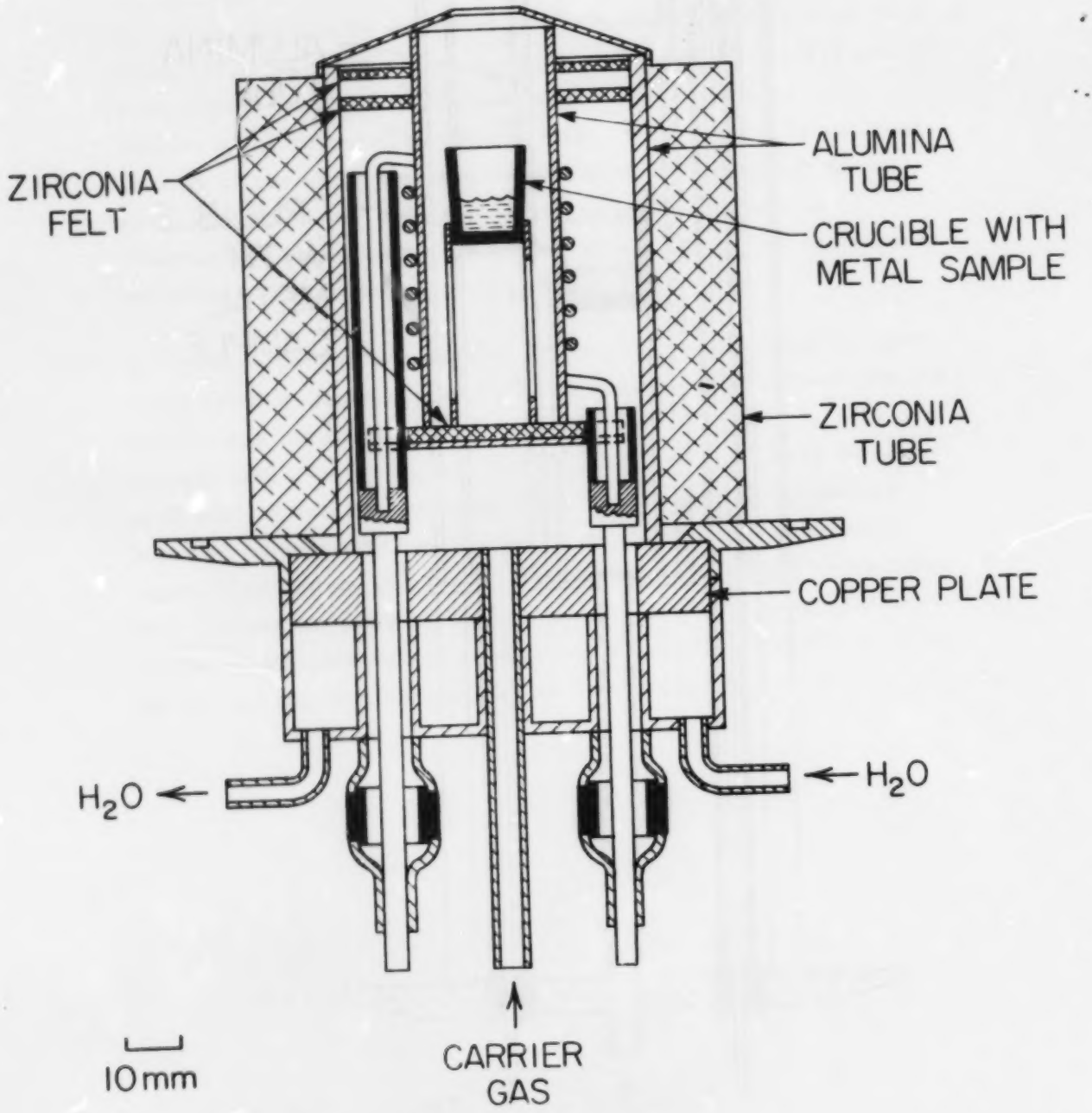

Fig. 3 High temperature furnace schematic.

SECTION IV

PLASMA-RESONANCE LIGHT SCATTERING FROM ALKALI METAL PARTICLES

INTRODUCTION

The first experiments performed under this grant investigated the light-scattering characteristics of particles made from alkali metals. The conduction electrons of the alkali metals are known to approximate a free-electron-gas model. One may calculate the scattering cross section for a small spherical particle using this model to supply the index of refraction as a function of wavelength.[13-17] The result is an anomalously large cross section at a particular light frequency which is resonant with the collective motion of the conduction electrons in the small particle. For the alkali metals this resonance occurs in the visible region of the spectrum. This phenomena of collective motion is called plasma-resonance and has been observed in various bulk metals by inelastic electron scattering, and by light scattering in thin films. However, the position (frequency) and width of this resonance should be a measurable function of particle size and shape, as well as composition. Plasma-resonance light scattering in small particles has been observed previously by various groups, but these experiments were the first observations made on particles that were forming <u>in situ</u> in free space and continuing to grow in size.

EXPERIMENTAL

Particles were formed using the standard furnace and vacuum apparatus described previously. Temperature of the furnace was adjusted empirically to obtain particle formation and measurements indicate metal equilibrium vapor pressures between 0.1 and 10 torr. Under typical operating conditions, metal was evaporated from the crucible at about 0.2 g/h. Lithium, sodium, and potassium were obtained commercially as sticks of 99.95% purity, packed under oil. Rubidium and cesium were obtained in glass vials with break-seal necks. The seals were broken from outside the furnace just before experiments were begun. Light scattering was observed by focusing light from a 450-W xenon arc lamp

directly into the observation chamber, and collecting the scattered light at 90° to the incident beam by a monochromator. Light from the monochromator was detected with a photomultiplier, and its intensity vs. wavelength displayed on a chart recorder. Greater detail of procedures and results is available in Ref. 18.

RESULTS

A weak resonance peak was observed for Lithium at 270 nm. Due to the weak signal no measurements of relative peak shift or width could be made. The high background of scattered light was attributed to reaction products of the liquid lithium with the alumina in the furnace as the alumina crucible was destroyed in less than 1 h of operation.

Two different resonant peaks have been observed with sodium particles: at 310 nm and at 400 nm. Subsequently to the published paper on these experiments it was found that the 310 nm peak is caused by the presence of a small amount of oxygen in the system. Therefore, contrary to the original published paper,[18] only the 400 nm peak can be considered as due to pure sodium particle plasma-resonance.

The 400 nm peak is easily observed and relative shifts in the peak were produced by changes in experimental parameters. A reduction in flow rate of the carrier gas (N_2) by a factor of 5 (from 2.5 to 0.5 cm^3/sec) was found to produce a shift of about 2 nm to a shorter wavelength. Pressure induced shifts were somewhat more pronounced. The "400 nm" peak shifts from 403.0 nm at 1.3 kPa to 384.0 nm at 4.0 kPa, both at a flow of 2.0 cm^3/sec (see Fig. 4). There was also a furnace-temperature dependence shifting from 385 to 419 nm as the temperature increased from 700 to 800 K at a constant flow of 2 cm^3/sec.

Attempts were made to obtain electron micrographs of sodium particles collected from directly above the furnace under conditions which gave sharp resonance scattering. The resulting photographs were not very

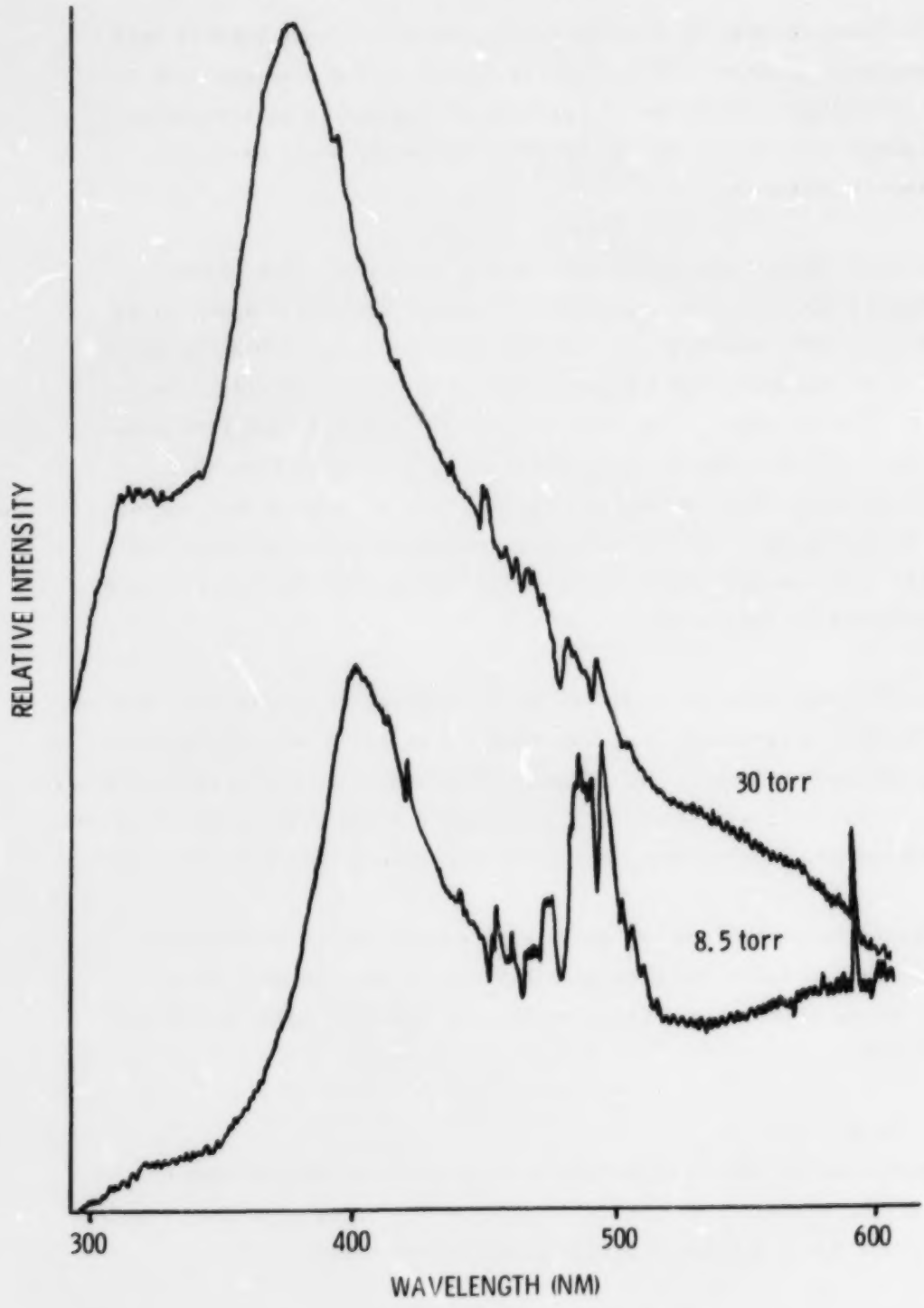

Fig. 4 Scattered light spectra of Na (uncorrected) at constant flow rate and furnace temperature showing the effects of increasing pressure. Curves have been displaced vertically for clarity.

definitive, apparently because the Na particles react rapidly with atmospheric moisture and are easily melted by the electron beam in the microscope. Definite correlation of changes in particle size and shape with shifts in the resonant frequency would have been extremely important.

Potassium behaved qualitatively similar to sodium. The plasma resonance for potassium particles is around 570 nm and appeared as an orange glow (see Fig. 5). As the pressure changed from 53 Pa to 267 Pa the peak shifted from 568.5 nm with a 42 nm width, to 577.0 nm with a 60.5 nm width. At constant pressure and flow rate the peak shifted from 571.5 to 558.0 nm and narrowed from 50.5 to 37 nm as the furnace temperature was lowered from normal operating temperatures ($\approx$ 600 K) to a point where no particles appeared. A weak peak was also recorded at 523.0 nm but this has not yet been satisfactorily explained.

Resonant scattering behavior was more difficult to obtain for rubidium particles. A resonance peak was observed at 625.0 nm (see Fig. 5) at a constant flow rate and furnace temperature and a pressure of 67 Pa. An increase in the pressure to 530 Pa shifted the peak to 631.5 nm and broadened it. Increasing the furnace temperature had a similar effect.

No resonance scattering was found with cesium vapor. Under some conditions, a faint red glow possibly due to Cs_2 was seen by eye. Very strong nonpolarized white scattering was seen under all normal conditions.

DISCUSSION

As mentioned in the introduction to this section the position of the plasma resonance may be calculated on the basis of a free electron gas model for a spherical particle of a given size:

$$w_R^2 = 1/3 w_p^2 \quad [1-3/2(w_p r)^2] \qquad (1)$$

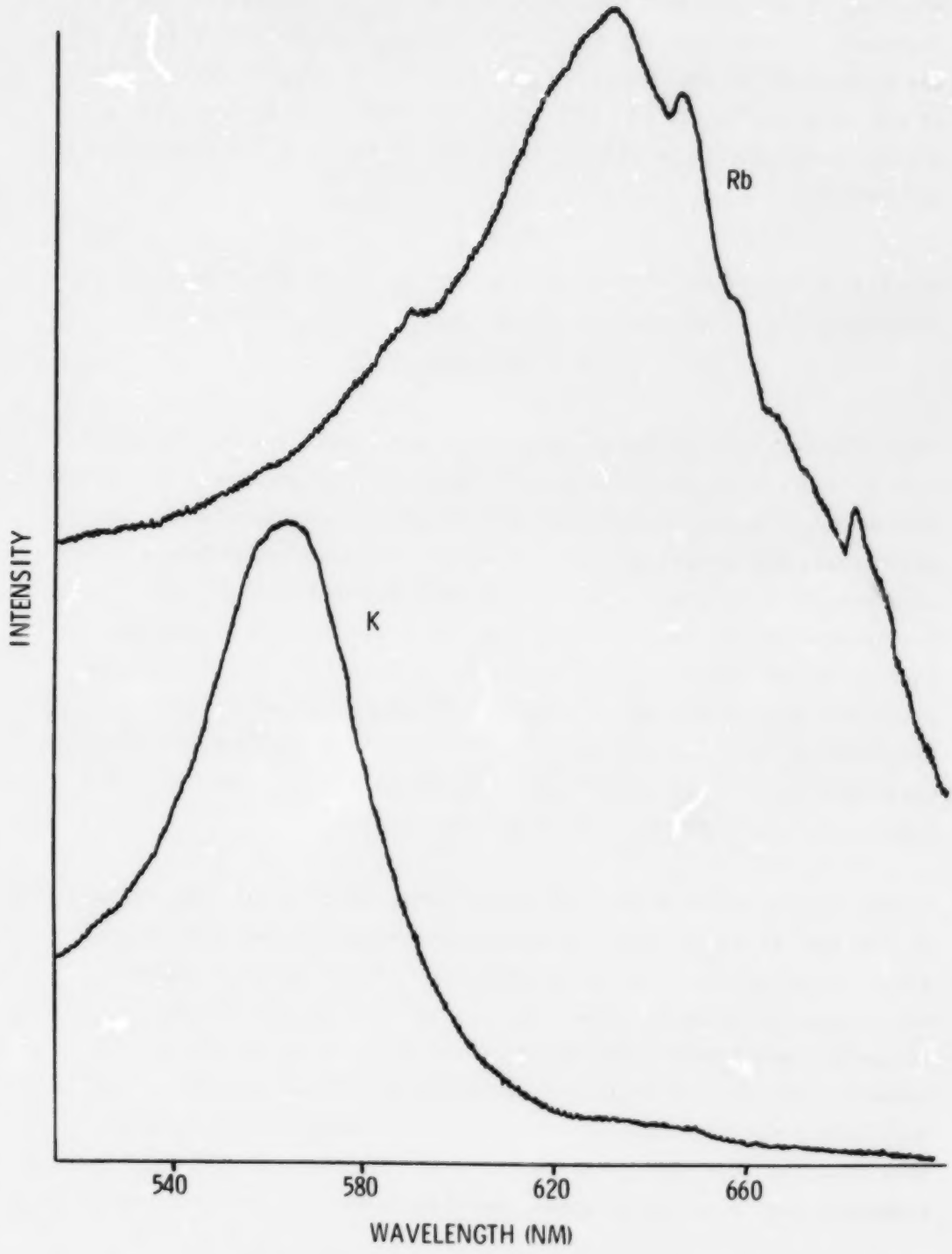

Fig. 5 Scattered light spectra of K and Rb, unreduced data. Curves displaced vertically for clarity.

where w_R is the resonant frequency, and w_p is the plasma resonance frequency for the bulk material. The relaxation time τ is related to the half-width of the observed resonance, $\Delta\lambda$, by $1/w_R\tau \approx \Delta\lambda/\lambda_R$. Since it may be argued that in a very small particle the mean free path of a free electron will be limited primarily by the walls of the particle and therefore:

$$\tau \approx R/V_F \tag{2}$$

where R is the radius of the particle and V_F is the Fermi velocity of the electrons. Eliminating τ and w_R from these equations gives:

$$R = 6\pi C V_F/\Delta\lambda w_p^2 \tag{3}$$

Table 1 summarizes the observed resonant peak positions of the alkali metals, and the expected wavelengths using Eq. 1 (λ_R-Calc). The second column gives the experimentally measured plasma wavelengths for the bulk metal, and column three is the calculated extinction peak resonance of a spherical particle with a 2.5 nm radius based on empirical measurement of the dielectric constant as a function of wavelength instead of the free-electron-gas model. Column five is the observed resonance wavelengths and illustrates the breakdown of the free-electron-gas model as the atomic number increases. Column six contains observed widths of the resonances, and the last column indicates the size of the particles as calculated from Eq. 2.

In the absence of an exact calcuation taking into account the effects of damping, it is difficult to accurately determine the size of the alkali metal spheres from scattering data. Radii given in Table I may be considered to be upper limits since the effect of other relaxation mechanisms would be to narrow $\Delta\lambda$ and give an artifically large R. The work of Doyle and Agarwal[19] calculated the extinction coefficient for particles from 2.5 to 40 nm radius. Their results show that for less than 10 nm radius there is only a slight shift of resonance peak position to longer wavelength but the peak narrows,

RESONANCE PEAK WAVELENGTHS AND PARTICLE DIAMETERS

(nanometers)

Metal	λ_p	λ_R (calc)	λ_{ext} (calc)	λ_{obs}	$\Delta\lambda_{obs}$	R
Li	155	269	...	270	...	...
Na	218	375	370	384 309	47	6.5
K	292	495	545	568 523	40	11.5
Rb	322	557	625	625	55	10
Cs	363	627	665	...	..	.....

Table 1. Summary of observed and calculated resonance peak wavelengths and minimum particle diameters. λ_p is the experimental bulk plasma resonance wavelength, λ_R is the resonance wavelength for a 5-nm spherical particle caclulated using Eq. 2, λ_{ext} is the extinction maximum for a 2.5 nm spherical particle (Ref. 14), λ_{obs} is the observed resonance maximum, $\Delta\lambda_{obs}$ is the observed resonance half-width, and R is the particle radius calculated from $\Delta\lambda_{obs}$ using Eq. 3.

as is expected from Eq. 3. Above 10 nm, the peak shifts more rapidly to longer wavelength accompanied by increasing half-width. No resonances which narrowed while remaining near the same wavelength were observed, implying that the smallest observed particles were greater than 5 nm. The prominent shifts of the resonances to longer wavelengths are interpretable as due to increasing particle size, while the relatively narrow resonance width indicates the formation of particles particles of uniform size.

SECTION V

ELECTRON MICROSCOPY OF Zn PARTICLES

GENERAL

Attempts at electron microscopy of the alkali metal particles led to consideration of other metals, as previous results indicated clearly defined crystalline forms with many other metals. Pb, Zn, Cd, and Mg have high enough vapor pressures to be used in the standard furnace and of these Zn, Cd and Mg yielded electron micrographs with clear crystalline shapes. Pb appeared to form small spheres with low contrast. None of these metals exhibits a plasma resonance frequency in the visible region of the spectrum. Zn was chosen for some extensive study and its plasma resonance was calculated to lie in the near ultra-violet, but has not yet been observed. Recent data[20] indicates that the resonance should occur in the vacuum UV at about 130 nm.

EXPERIMENTAL

The furnace and vacuum apparatus used in these experiments was the same as in the alkali metal experiments with the addition of a butterfly valve to the main chamber to facilitate electron microscope samples (see Fig. 6).

Sample collections were taken on a thin Parlodian plastic film supported by standard electron microscopy 200-mesh copper grids of 3-mm diameter (corresponding to ≈ 0.1-mm squares). Grids were mounted on the tip of a movable 3-mm stainless steel rod. The rod served as an adjustable feedthrough to the outside of the system and was sealed with rubber O-rings so that the rod and grid assembly could be slipped into and out of the observation region without introducing an air leak into the vacuum (Fig. 6). During a typical experiment of 2 or 3 h, up to 20 samples would be taken by using the side chamber as an air lock, so that the main system was unaffected by changing grids. Collection times were varied according to the position in the chamber and flow

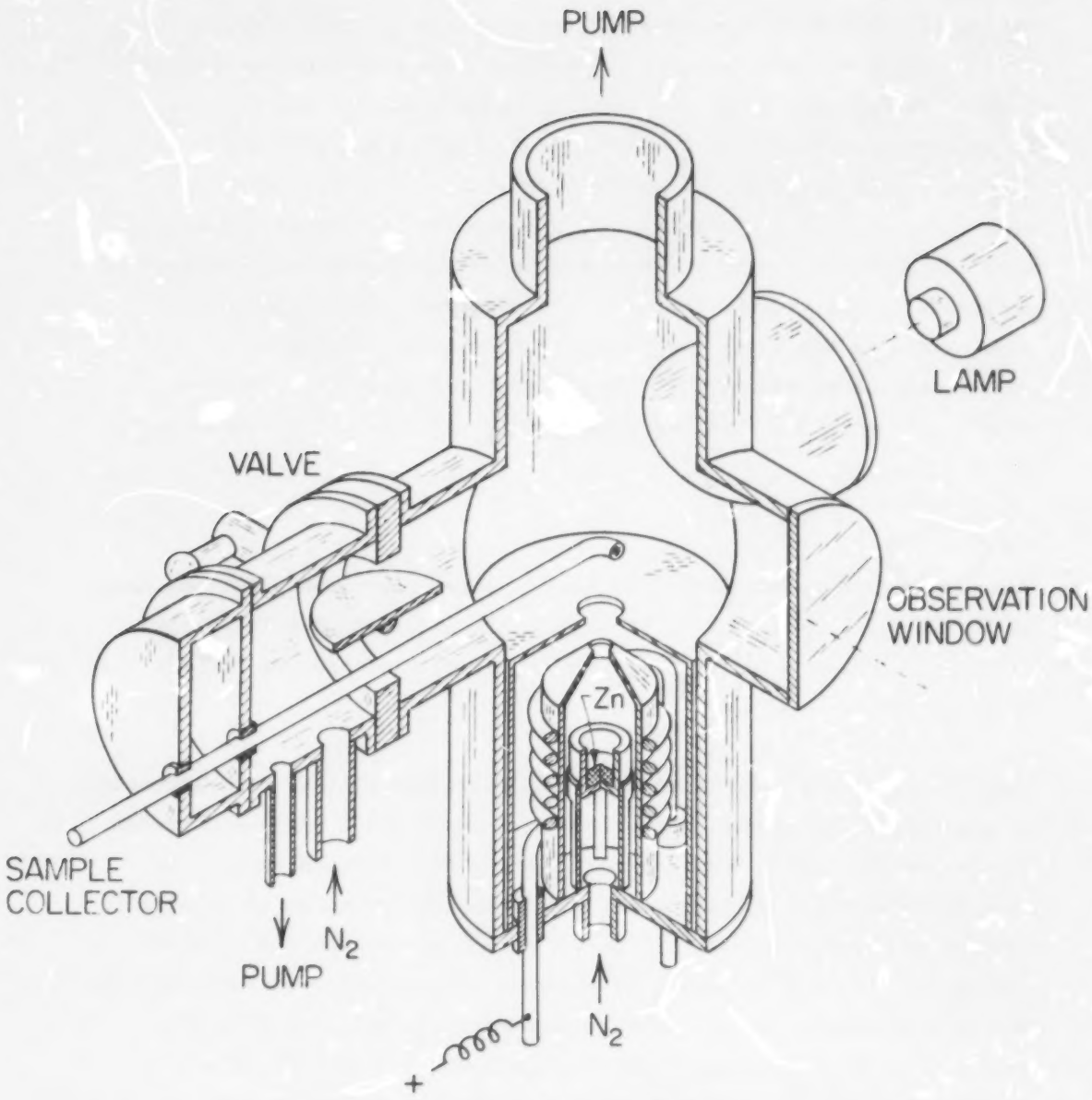

Fig. 6 Observation chamber and particle collecting apparatus schematic.

conditions. Most collection times were from 1-4 min with shorter times at close distances to the nozzle. The mounted grid was maintained in the side chamber with the valve closed until it was ready to be moved into position for collection.

When the collection was completed, grids were taken to the electron microscope and scanned at low magnification for evidence of deposit. Higher magnifications (up to 50,000 X) were used for observation and transmission photography. Some 150 samples were collected in this study, and typically 3 or 4 photographs were taken to characterize each sample. Reference 21 is a paper published on many of these experiments.

RESULTS

Samples were obtained with variations in carrier gas flow rate, furnace temperature, pressure, and position in the observation chamber. It was hoped that a correlation of particle characteristics to one of these variables would be evident. However, changing something like the flow rate was found to modify all of the physical parameters of the system (such as, supersaturation ratio, initial atom concentration, etc.). Therefore, an exact prescription of the physical parameters needed for control of nucleation was not developed. The critical factor in determining the size of the particles was time, or the age of the particles.

On the basis of frequency of occurrence, the most probable shape of the observed Zn particles is described as a section of a regular hexagonal prism. The particles had two stable orientations on the parlodian plastic. These two orientations are designated the "end-on" and "side" views corresponding to hexagonal and rough rectangular silhouette, respectively. Figure 7 is an example of some large particles ($\approx$ 1200 nm diameter), two of which show a layered rectangular side shape.

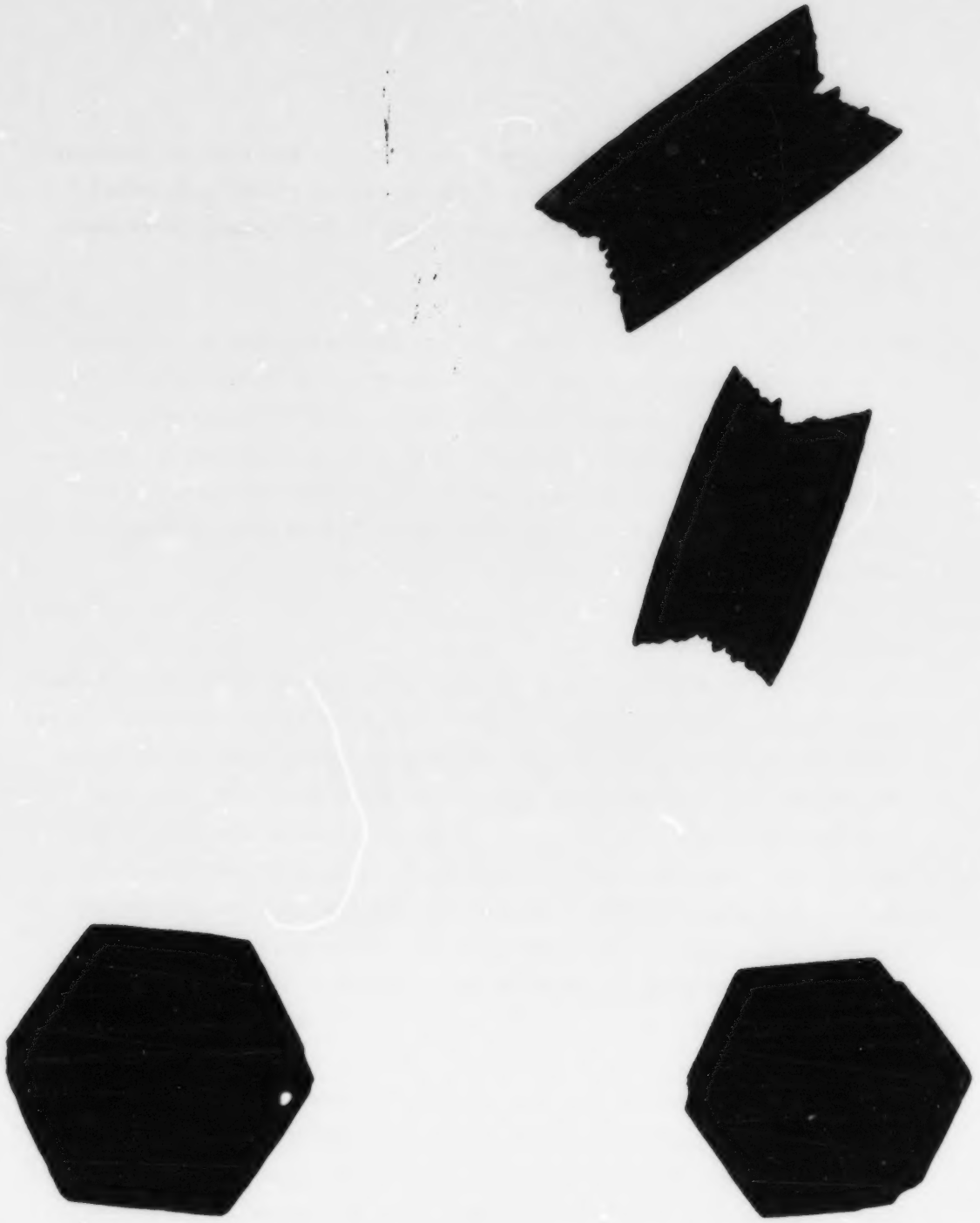

Fig. 7 These particles are single Zn crystals about 1200 nm across. The two hexagons represent "end on" views, while the other two have the same shape but are rotated out the page by 90° to present a "side view (6000 K).

Electron diffraction on one single hexagon indicates that the central axis of the hexagonal prism is perpendicular to a simple crystallographic plane. The hexagonal cross section occurs in all the samples taken (excepting cases of contamination).

Other shapes also occur, such as triangles, irregular hexagons and pentagons. The triangular shape is consistent with the hcp structure of bulk Zn; it commonly appears, but is always less abundant than the hexagon. If one expects the particles to approach a spherical shape, the triangular shape of viewed as a possible but less probable configuration.

As the size of the particle increases, the sides of the hexagonal prism usually becomes indented, which results in an hourglass- or butterfly-shaped side view as in Figs. 7 and 8. Particles ranging in size from 20 to 500 nm appear to be layered.

In Fig. 9 are three-dimensional sketches with corresponding side views, summarizing the various shapes and size groups of the observed particles. The smaller particles were found at short times (distance/flow rate) form the tip of the nozzle, typically within 1-3 cm, while the larger particles were found at greater distances. The collected particles were generally very uniform, with sizes varying by a factor of 3. Some pictures show two distinct size populations separated by an order of magnitude. Eddy currents and lack of laminar flow in the collection region could account for this variation.

The largest sized particles (500 to 5000 nm diameters) were usually identifiable as an agglomeration of smaller particles. However, it was not always obvious whether a particle was a composite or a single crystal. The striking effect with the larger particles is that they usually retain the basic hexagonal prism shape.

Fig. 8 Indented or butterfly side views typical of medium sized (100 nm diam.) hexagons (40,000 x).

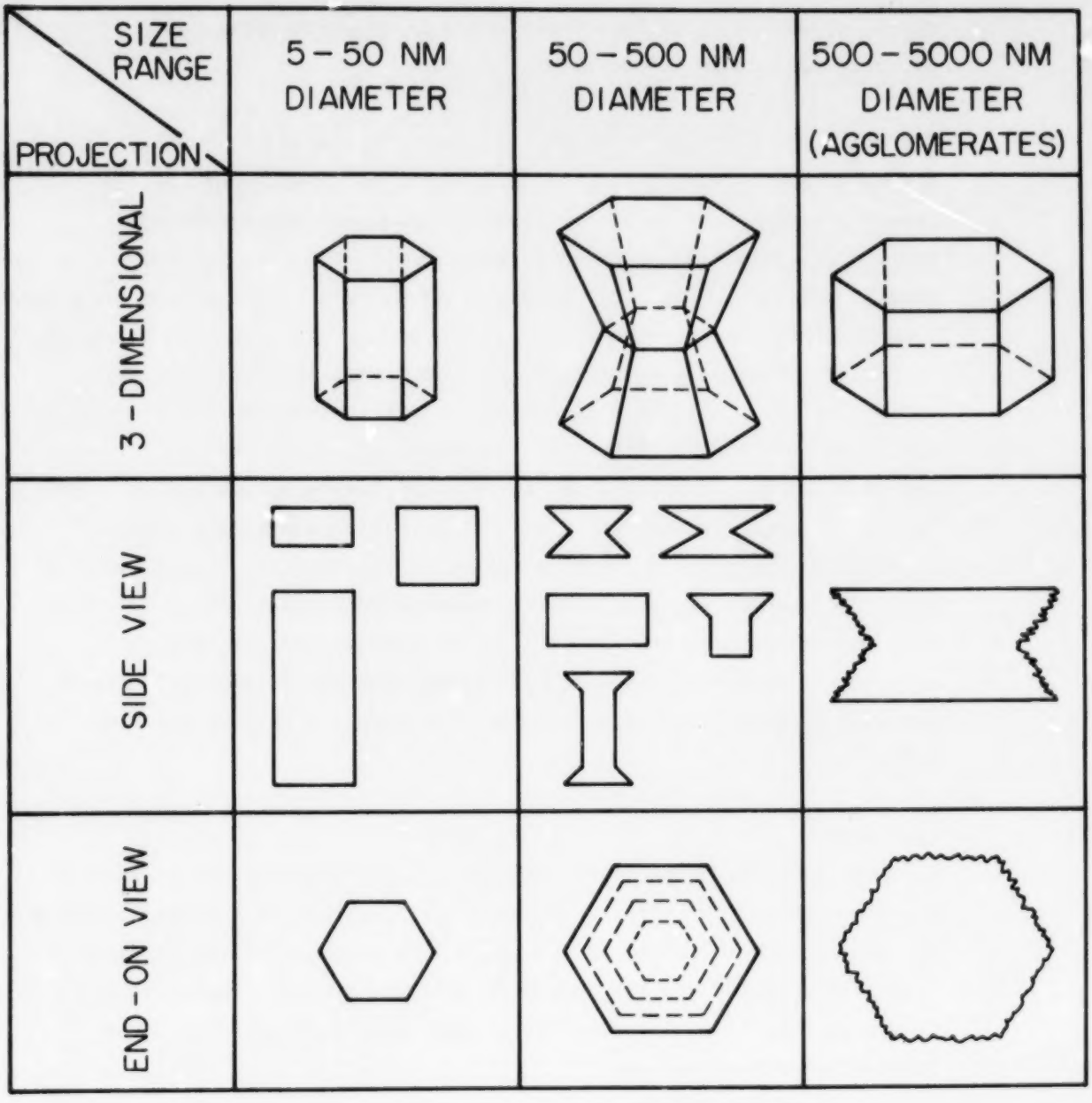

Fig. 9 Summary of the three observed size categories of hexagonal-plane particles and corresponding general shapes in three-dimensional, end-on, and side projections.

Figure 10 is a clear example of an agglomerated particle with hexagonal shape made from smaller hexagonal prrticles. This phenomenon is an example of agglomeration that occurs in the gas phase, since under normal operating conditions there are some discrete particles directly visible in the observation region.

The deleterious effect of O_2 on the crystalline shape of the particles, described previously by several investigators,[6-8] was confirmed in this system by means of an air leak. Unless care was exercised in the sample collection process, a small amount of air would yield results similar to Fig. 11. A careful study of the effect of controlled amounts of O_2 has not been made, but the oxygen may coat the nucleated particles epitaxially and thereby prevent further growth except by agglomeration. This suggestion follows from the observation that light scattered from the particles becomes highly polarized when O_2 is introduced into the collection region. Complete polarization at a 90° scattering angle is associated with the Rayleigh scattering limit of very small particles (small compared to wavelength). Also, isolated particles were rarely observed in contaminated samples; however, when they occurred they were always 5 nm or less in diameter (Fig. 11). Diffraction patterns of such contaminated samples are similar to those obtained with pure crystals, but detailed comparisons have not been made.

DISCUSSION

The most probable shape of the observed Zn particles has been explored in some detail. It basically consists of a section of a hexagonal prism, but as illustrated in Fig. 9 the shape is a function of the absolute size of the particle. In the growth or aging process, agglomeration is a significant mechanism and it becomes more pronounced at higher furnace temperatures.

Since a considerable amount of theoretical work is available on

Fig. 10 Good example of a single large (400 nm) particle agglomerated from (20 nm) hexagonal particles in the gas phase (40,000 x).

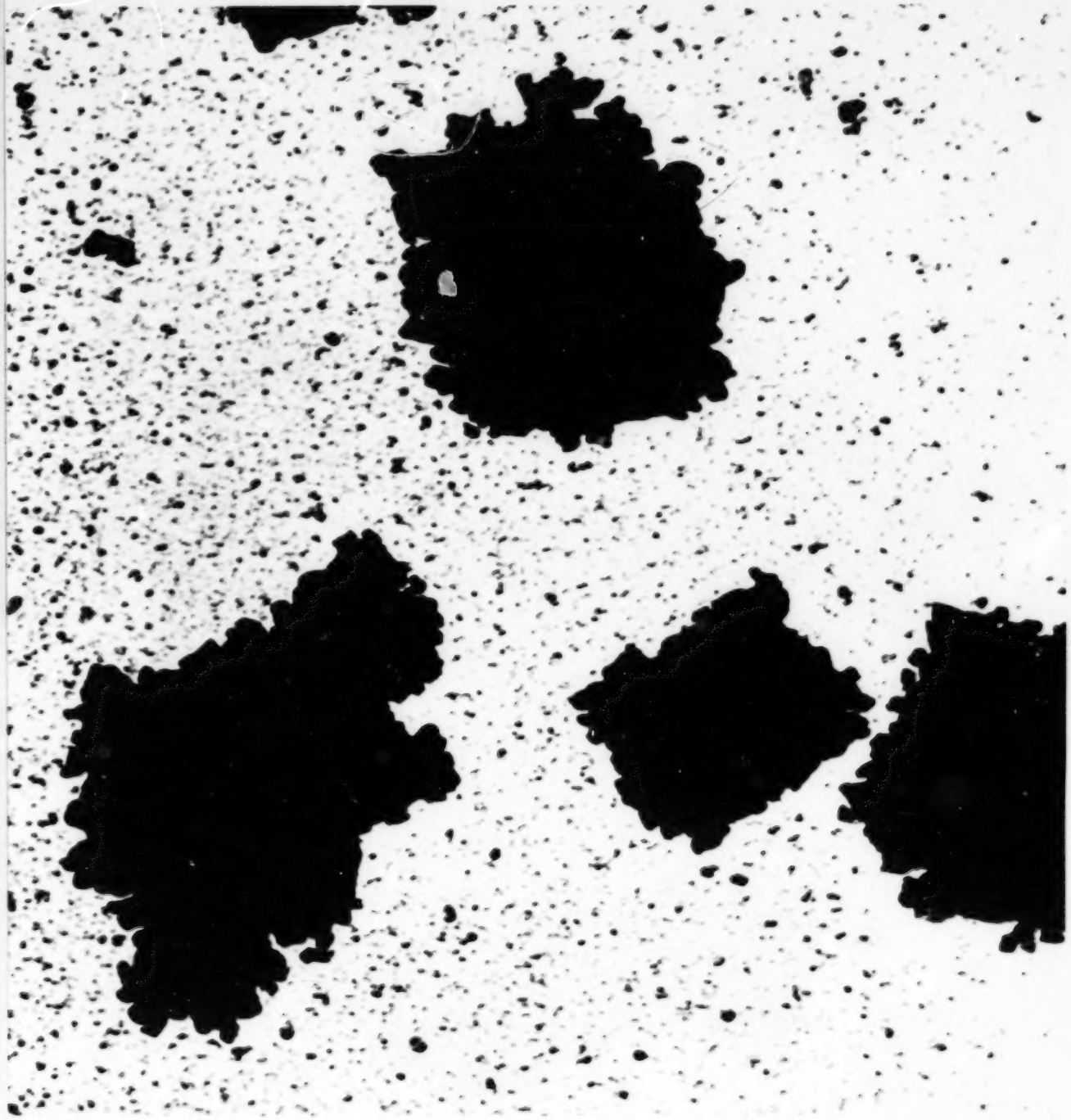

Fig. 11 O_2 contaminated sample showing the pronounced tendency for particles to clump together. The single particles are 5 nm or less in diameter, while the large clumps are on the order of 500 nm across (40,000 x).

homogeneous nucleation, information concerning the nucleation of these small crystals is of interest. From this point of view, further studies with the electron microscope seem inadequate. The smallest particles observed with our instrument were on the order of 5 nm in diameter Fig. 12 which corresponds to about 10,000 atoms by using the density of bulk Zn. However, at this magnification, measuring the diameter on the photograph only puts an upper limit to the actual size. This is consistent with the specifications of our electron microscope, which in principle can detect a particle of 1 nm diameter. In order to adequately study the structure of a particle, its diameter must exceed this minimum resolution by an order of magnitude. Figure 12 illustrates this conclusion; the smallest clearly shaped hexagons are about 10 nm across. Electron diffraction analysis and other electron microscopy techniques can be applied to yield much more information, but it would be very desirable to discover in situ methods of analysis as well. Theoretical considerations give a relation for the smallest size of stable particle in terms of the ratio of the actual metal vapor pressure to the equilibrium vapor pressure at the same temperature, known as the supersaturation satio. As the supersaturation ratio increases the smallest size for a stable particle decreases. The temperatures in the collection chamber yield supersaturation ratios of roughly 100-1000. These numbers predict a smallest size of particle containing on the order of 10 atoms, which points out the inadequacy of using the electron microscopy exclusively to probe nucleation. Thus, results remain at a qualitative level. The uniformity of sizes in a given sample encourages the idea that quantitative measurements can be compared to theoretical calculations. Time may be parametrized by distance in the flow system to allow a measurement of rates of nucleation and growth.

Fig. 12 Example of the smallest size range of particles (5-20 nm diameter) for which clear geometric shapes were resolved (160,000 x).

SECTION VI

SMALL PARTICLE JOSEPHSON MAGNETOMETER

Use of electron tunneling effects in small particles at low temperature was viewed as a possible new way to determine size and size distribution. Measurements were made on thin film, stable arrays with large numbers of small selenium particles produced by evaporating the metal in an inert gas at low pressure. Particle sizes as revealed by electron microscopy ranged from 10 to 1000 nm, but were usually uniform and typically centered around 200 nm. These arrays showed potential for investigation of phase coherence properties of large numbers of coupled junctions and also for application as reliable, sensitive magnetometers. Reference 22 contains many of the experimental details.

Samples with resistances less than 100,000Ω/square all had nonzero critical currents below 3.77 K. The critical currents varied as R^{-n} where R is the resistance and $n = 1.5 \pm 0.2$ with a 1 K /square sample having a critical current of approximately 50 μA. The nonzero voltage part of the I(V) curve could be hysteretic or not depending on sample resistance, temperature, and particle size. For particles formed in 100 μ air, samples with resistances above 500 Ω/square were not hysteretic at any temperature (down to 1.07 K) for bias voltages less than a few mV. Lower resistance samples would be nonhysteretic near their transition temperature but become hysteretic as the temperature was lowered.

A simple model[22] can be used to explain perhaps the most interesting characteristic of these samples, their response to magnetic fields. Figure 13(a) shows that the critical current is a multiply periodic function of a magetic field applied perpendicular to the plane of the array.

The critical current, I_c, was monitored by applying a d.c. bias current just less than I_c and an a.c. modulation current large enough so

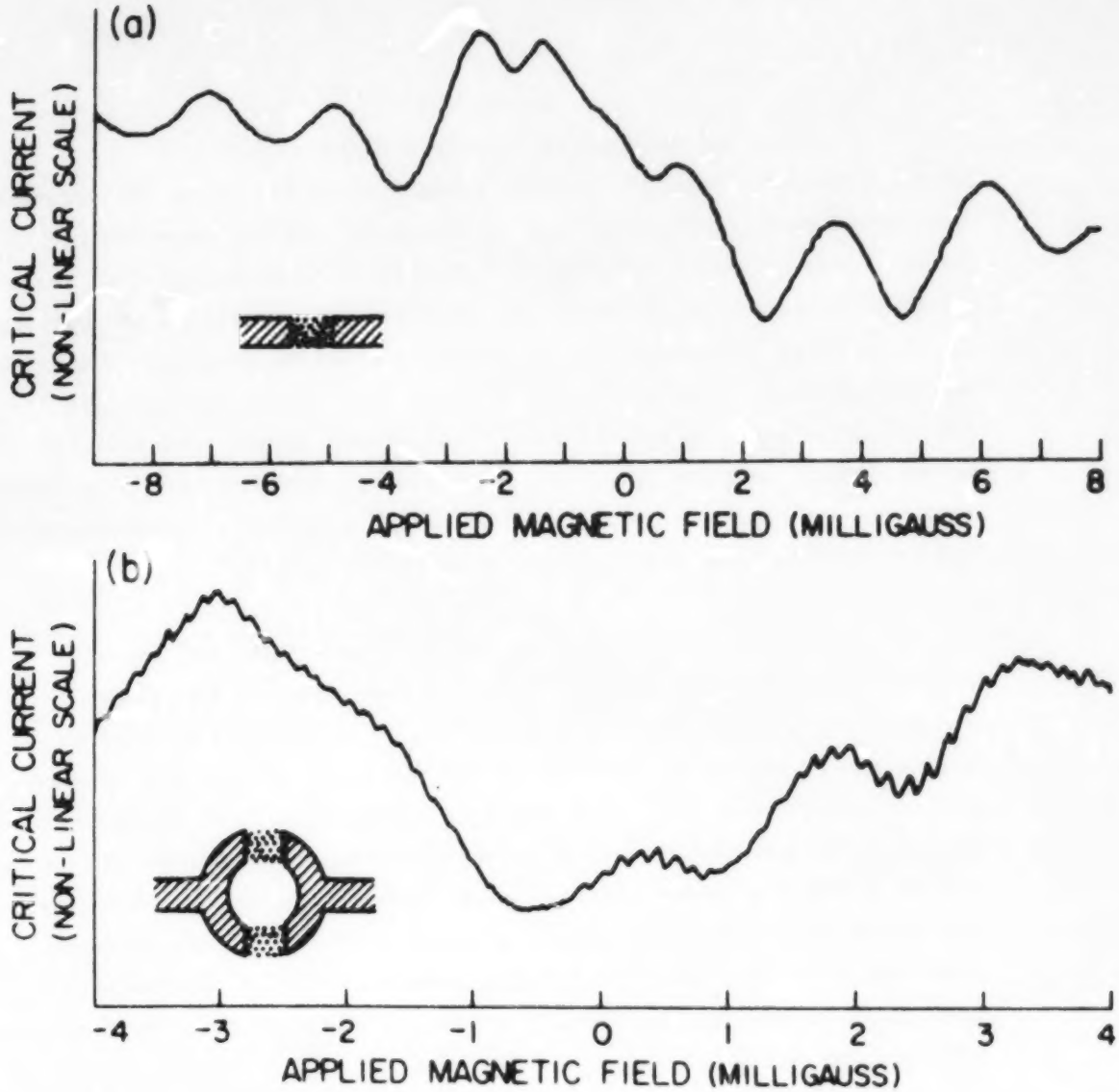

Fig. 13a The magnetic field dependence of the critical current of a small particle array 0.32 mm long x approximately 0.03 mm wide that was cut with a scribe from a wider film of small particles. The amplitude of the most rapid periodicity is approximately 0.4 μA.

Fig. 13b The magnetic field dependence of the critical current of two coupled small particle arrays, each 0.32 mm long x approximately 0.05 mm wide. The most rapid periodicity has an amplitude of 0.24 μA and a magnetic flux period of $2.1 \pm 0.2 \times 10^{-7}$ g cm^2.

that I_c was exceeded during part of each a.c. cycle. The a.c. voltage across the sample, which was measured with a lock-in amplifier, is a non-linear measure of I_c. The non-linearity was due to the fact that the dynamic resistance for $I > I_c$ is a non-linear function of I. The most rapid magentic field periodicity is on the order of Φ_0/A where A is the area of the array and $\Phi_0 = h/2e$ is one flux quantum, but many longer periodicities, up to over 100 Φ_0/A for a typical sample, are present.

The probable explanation is that the many periodicities result from quantum interference effects[23] around the many loops formed by pairs of current paths. The largest area loop, defined by the outermost current paths, would be expected to be of the order of the sample area.

As an example, unambiguous measurements of the magnetic flux periodicity could be made with a double junction geometry shown schematically in the insert of Fig. 13(b). For these samples, a magnetic field period Φ_0/A_ℓ is the loop area, was observed superimposed on an envelope with periodicities $\geq\Phi_0/A$, where A is the area of the individual arrays. (Analogous to a double slit diffraction pattern with finite slit width.) Figure 13(b) shows experimental results for the best sample. Other samples had the same general features, but the amplitide of the rapid periodicity was smaller. Probably this was due to inequality in the critical currents through the two arms. The mean flux period for samples of this geometry was 2.0×10^{-7} G cm^2 with a standard deviation of 0.2×10^{-7} G cm^2 ($\Phi_0 = 2.07 \times 10^{-7}$ G cm^2).

For use as magnetometers, the typical sensitivity of good samples was a few parts in 10^{-5} G with a 1 sec time constant. Some samples had sensitivities as great as a few parts in 10^{-6} G. One very small area sample had a magnetic flux sensitivity of 1.5×10^{-4} Φ_0. The sensitivities obtained now, though not comparable to those of the best superconducting devices,[24] are adequate for a wide range of applications.

The arrays have not degraded with room temperature storage and survive frequent thermal cycling with no protection from condensed atmospheric moisture.

In summary, we have produced and studied arrays containing $\approx 10^6$ small, weakly coupled particles each $\approx$200 nm in diameter. The I(V) and $I_c(H)$ characteristics can be qualitatively understood with a simple model which simulate the array by a set of n current paths in parallel, each with m Josephson weak links in series. The arrays show potential as practical magnetometers in that they are easy to fabricate, operate with d.c. electronics, and presently have sensitivities of a few parts in 10^{-5} G.

SECTION VII

OBSERVATIONS OF LAMINAR FLOW IN A GLASS TUBE

One of the unique characteristics of this system of nucleating particles is that it occurs in a steady flow. Eddy currents in the particle flow are readily observed in the apparatus described previously. However, if these eddy currents could be eliminated then an obvious step would be to look at light scattering from different points downstream. A glass tube (10 cm diameter) was devised for this purpose to replace the observation chamber cross. Since there were no irregularities in the wall surface, no eddy currents were formed and the particle flow was unidirectional up the tube. However, deposition by diffusion gradually clouded the walls. Further attempts added more gas flows to keep the walls clean, but these resulted in unstable oscillatory particle flows. Stable flows with unclouded walls never exceeded more than about 30 minutes of experiment time. Data that was obtained did not indicate a detectable consistent change as a function of distance along the glass tube. Nucleation and growth seem to occur close to the furnace exit, and in terms of the plasma-resonance are not large effects further downstream. The glass tube apparatus also allowed the possibility of 0-180° angular light scattering from the particles. However, this experiment was never initiated due to the large amount of computer and programming time required for data reduction coupled with the small amount of expected information.

SECTION VIII

"MATRIX" ISOLATION OF Na PARTICLES

The isolation and entrapment of small particles was pursued as a technique to facilitate other experiments such as Raman laser scattering, NMR, and ESR. This was accomplished by a cryogenic method of freezing the particles and carrier gas to a solid. The particles and carrier gas are exposed to a cold ($\approx$ 20 K) copper plate. Gas coming in contact with the plate will undergo a phase change to the solid state. The metal particles originally in the gas will be entrapped in their "matrix" of frozen gas. Since particle apparatus and the cryogenic apparatus required greatly different gas pressures, a "pulsed" technique was employed for matrix deposition. A large valve connecting the two systems was opened for short periods of time ($\approx$ 1 sec) with long intervals in between to allow the cryogenic system to restabilize. Although matrix deposition was observed, and particle entrapment was indicated by weak plasma resonance light scattering, a good thick matrix was never obtained. After just a few deposition pulses, no further deposition occurred. Since the temperature of the cryotip copper plate continuously rose during deposition it was concluded that the cryogenic apparatus did not have sufficient power dissipation to adequately carry out such experiments.

SECTION IX

RAMAN SCATTERING

Initially, observation of Raman scattering from particles illuminated by an Argon ion laser beam (1 watt) was attempted *in situ*. No Raman signals were observed and estimates of the particle density above the furnace (10^{10} - 10^{13}/cc) indicated that this would be a difficult approach assuming that the Raman cross section of the particles was comparable to that of N_2 or O_2 gas. Therefore further attempts employed the matrix isolation technique of collecting the particles in a larger concentration than the gas phase. Various lines of a 1 watt Argon ion laser were focused onto the matrix of particles, and a scanning double monochromator with a low-noise phototube was employed for detection but no lines attributable to the particles were observed.

SECTION X

SUMMARY

Studies performed under this grant strongly indicate that plasma resonance light scattering may be a significant tool for obtaining data on the subject of homogeneous nucleation. Plasma resonance peaks and widths for alkali metal particles have been observed to change systematically with system parameters; and electron microscopy of Zn and other metal particles has revealed sizes and characteristic geometric shapes. Correlation of these observations may result in determination of size and/or shape of small particles by careful measurement of the position and width of the plasma resonance. This, in turn, would directly provide information to compute nucleation and growth rates in a steady-state system. Information on particle formation obtained for metals with a plasma resonance could be generalized to other substances.

SECTION XI

REFERENCES

1. Report of the National Bureau of Standards Study Group on Air Pollution, Measures of Air Quality Program (National Bureau of Standards, 1970).

2. Project Clean Air Task Force Assessments (University of California 1970).

3. Air Quality Criteria for Particulate Matter, National Air Pollution Control Administration Publication AP-49 (1969). Over 300 references listed here.

4. Air Pollution Engineering Manual, Public Health Service Publication No. 999-AP-40 (1967).

5. Control Techniques for Particulate Air Pollutants, National Air Pollution Control Administration Publication No. AP-51.

6. L. Silverman, Air Repair 4, 189 (1955).

7. E.R. Frank and J.P. Lodge, J. Microscopie 4, 449 (1967).

8. T.A. Rich, L.W. Pollak and A.L. Metnieks, Geofis. Pura. Appl. 44, 233 (1959).

9. W.J. Megaw, J. Rech. Atmopheriques 2, 53 (1966).

10. C. Orr, F.K. Hurd, W.P. Hendrix and C.E. Junge, J. Meteorol. 15, 240 (1958).

11. Task Group on Lung Dynamics, Health Physics 12, 173 (1966).

12. West, J.B., Bradford, R.S. Jr., Eversole, J.D., and Jones, C.R. Rev. Sci. Instr. 46, 164 (1975).

13. S. Yamaguchi, J. Phys. Soc. Japan 15, 1577 (1960).

14. D.P. Gilra, Collective Excitations in Small Particles and Astronomical Applications, Ph.D. Thesis, University of Wisconsin 1972.

15. W.T. Doyle, Phys. Rev. 111, 1067 (1958).

16. M. Kerker, The Scattering of Light and Other Electromagnetic Radiation (Academic, New York, 1969).

17. H.C. Van de Hulst, Light Scattering by Small Particles (Wlley, New York, 1957).

18. D.M. Mann and H.P. Broida, J. Appl. Phys. 44, 4950 (1973).

19. Doyle, W.T. and Agarwal, A., J. Opt. Soc. Am. 55, 305 (1965).

20. Mosteller, L.P. Jr., and Wooten, F., Phys. Rev. 171, 743 (1965).

21. Eversole, J.D. and Broida, H.P. J. Appl. Phys. 45, 596 (1974).

22. Hansma, P.K., Sol. State Comm. 13, 397 (1973).

23. References and a comprehessible summary are given by Mercereau, J.E., Superconductivity (ed. by Parks, R.D.) Marcel Dekker, New York (1969).

24. An excellent summary of work on these devices is contained in several articles in the special issue of Proc. IEEF on Cryogenics, published January 1973.

SECTION XII

LIST OF PUBLICATIONS

1. D.M. Mann and H.P. Broida, J. Appl. Phys 44, 4950 (1973).
2. P.K. Hansma, Sol. State Comm. 13, 397 (1973).
3. J.D. Eversole and H.P. Broida, J. Appl. Phys. 45, 596 (1974).